Propagation and reflection of internal waves

B. R. Sutherland[a)]
Department of Mathematical Sciences, University of Alberta, Edmonton, Alberta T6G 2G1, Canada

(Received 24 June 1998; accepted 20 January 1999)

Fully nonlinear numerical simulations are performed to examine the behavior of large-amplitude internal gravity waves incident upon a level where the Doppler-shifted frequency of the waves is comparable to the background buoyancy frequency. Although linear theory predicts that the waves should reflect if the Doppler-shifted frequency is greater than the buoyancy frequency, it is found that nonlinear effects may greatly enhance the transmission of a wave packet across a reflecting level. If the Doppler-shifted frequency is moderately less than the buoyancy frequency, then nonlinear effects may greatly enhance the reflection of waves. A range of simulations is performed to characterize the reflection coefficient as a function of the amplitude and spatial extent of the wave packet. In comparison with horizontally periodic wave packets, it is found that the nonlinearly enhanced transmission of wave packets is more significant if they are horizontally compact. This occurs because the wave-induced mean flow effectively increases and decreases the horizontal phase speed of the waves on the incident and trailing flank of the wave packets, respectively, and this significantly broadens the frequency spectrum of the waves. © *1999 American Institute of Physics.* [S1070-6631(99)01205-2]

I. INTRODUCTION

An internal wave is a disturbance propagating under the effects of buoyancy in a fluid whose density varies with height. These waves are known to transport momentum and energy vertically through the atmosphere and ocean, and they may constitute a significant source of drag to the mean flow at levels where they break or dissipate. A great number of studies have been devoted to understanding the behavior of internal waves as they approach a level where the mean-flow speed is comparable to the horizontal phase speed of the waves (e.g., Bretherton,[1] and recently Winters and D'Asaro,[2] Lombard and Riley.[3] Also see Lighthill,[4] Sec. 4). This is known as the ''critical level.'' In theory and as numerical simulations demonstrate, as internal waves approach a critical level their vertical wavelength decreases to infinitesimal size and their amplitude increases. Eventually, the waves either dissipate or break, and deposit momentum to the mean flow. If, as is often the case for topographically generated waves, the horizontal phase speed of the waves is less than the mean-flow speed, then a drag is exerted on the mean flow near the critical level.

Less well studied is the circumstance in which internal waves encounter a level where the density is almost uniform. In this case, the waves are expected to reflect. More generally, waves are assumed to reflect from a level where their Doppler-shifted frequency equals the background buoyancy frequency.[1,5,6] This is referred to hereafter as a ''reflecting level,'' which is distinct from a critical level. In theory, as internal waves approach a reflecting level, their vertical wavelength increases. Beyond the reflecting level the waves are evanescent, their amplitude decreasing exponentially with distance from the level. Rigorously, the structure of an internal wave at a reflecting level—a ''caustic''—is given by linear theory in terms of an Airy function.[4] Linear theory assumes that the waves are monochromatic and small amplitude. The theory may be applied to small-amplitude wave packets with a broad frequency spectrum by applying the superposition principle. However, the behavior of large-amplitude internal waves at a reflecting level is not so well understood.

Here we examine the transmission and reflection of internal waves across a reflecting level by way of numerical simulations employing the fully nonlinear equations of motion. This work is a continuation of the studies by Sutherland,[7] who examined the propagation in nonuniformly stratified stationary flow of horizontally periodic internal waves incident upon a level where the background buoyancy frequency is comparable to the frequency of the incident waves. Therein it was shown that for vertically compact wave packets, depending on whether the stratification decreases greatly or moderately at a given level, weakly nonlinear effects act either to enhance or diminish, respectively, the transmission of internal waves into regions where the buoyancy frequency is small.

The weakly nonlinear effects are related to what has been called the ''self-acceleration'' of internal waves (e.g., see Grimshaw,[8] Fritts and Dunkerton[9]). For a horizontally periodic, vertically compact wave packet, its phase speed changes due to wave, mean-flow interactions.[7] For example, consider an upward propagating wave packet whose amplitude decreases with height. At the leading edge of the wave packet the mean flow accelerates due to the divergence of its associated momentum flux. If the waves are of large amplitude, the acceleration may be sufficiently large that the wave-

[a)]Fax: (780) 492-6826; phone: (780) 492-0573; electronic mail: bruce.sutherland@ualberta.ca; web: http://taylor.math.ualberta.ca/~bruce

 © 1999 American Institute of Physics
This article is copyrighted as indicated in the article. Reuse of AIP content is subject to the terms at: http://scitation.aip.org/termsconditions. Downloaded to IP: 129.128.216.34 On: Sun, 23 Mar 2014 03:22:20

induced mean flow is comparable to the horizontal group velocity of the wave packet. In this case, the horizontal phase speed along the leading edge of the waves increases. Likewise, along the trailing edge of the wave packet the mean flow decelerates and the horizontal phase speed of the waves decreases. As a consequence of symmetry, the horizontal wavelength of horizontally periodic waves does not change over time. Therefore as the phase speed of the waves increases and decreases, the frequency increases and decreases, respectively.

In the absence of dissipation, wave breaking or other nonconservative processes, the transient passage of the wave packet across a fixed vertical level has no permanent effect upon the mean flow at that point.[10,11] However, the effective changes in the wave frequency due to the self-acceleration of the waves can significantly affect the behavior of a wave packet incident upon a reflecting level. Sutherland[7] showed that as a large-amplitude wave packet approaches a reflecting level the relative changes in the wave frequency become larger. Due to the superposition of the incident and reflecting waves, the amplitude of the disturbance increases by as much as double that of the incident wave packet. Correspondingly, the changes in phase speed at the reflecting level can be four times as large. These changes can act to enhance the transmission of internal waves across the reflecting level in the following way: as the waves reflect, the frequency of the waves at the trailing edge of the incident wave packet decreases, and if this reduced frequency is smaller than the buoyancy frequency above the reflecting level, then a propagating wave packet is transmitted beyond the reflecting level. The wave packet has larger amplitude than one would predict on the basis of linear transient effects alone.

If no reflecting level exists, weak nonlinearity may nonetheless affect the transmission of internal waves if the buoyancy frequency is comparable to but greater than the Doppler-shifted frequency of the incident wave packet. In this case, because the phase speed of the waves on the incident flank of the wave packet increases, the frequency increases. If the buoyancy frequency is smaller than the increased frequency, a proportion of the wave packet reflects that is larger than that predicted on the basis of linear transient effects.

In this work, we extend these results to consider the behavior of a wave packet that is both vertically and horizontally compact, and which is propagating in a uniformly stratified shear flow. A fundamental change in dynamics is expected to occur as a result of the breaking of the horizontal translational symmetry. Whereas a horizontally periodic wave packet is capable of accelerating the mean flow either transiently due to wave–wave interactions, or permanently due to wave, mean-flow interactions or dissipation, a horizontally compact wave packet cannot directly affect the mean flow. Such a wave packet is capable of accelerating only the background flow across the extent of the wave packet itself. It is shown that for large-amplitude internal waves this horizontal nonuniformity significantly enhances the wave dispersion. As a result, the frequency spectrum of the wave packet greatly broadens. As this wave packet propagates in a shear flow toward a reflecting level, the proportion of the incident wave packet that is transmitted may be greatly enhanced or diminished.

In Sec. II the details are given of the numerical model used to simulate the propagation of internal waves. Section III first shows the results of simulations of horizontally periodic and horizontally compact wave packets in uniformly stratified stationary fluid. These control studies demonstrate the effect of self-acceleration upon the wave structure. The results are then shown of simulations of internal waves propagating in uniformly stratified shear flow. The spectra and characteristics of the reflected and transmitted waves are analyzed. In Sec. IV, the reflection coefficients are calculated for a range of simulations of small- and large-amplitude wave packets with different horizontal extents. A summary of these results and their implications to atmospheric and oceanographic modeling are given in Sec. V.

II. NUMERICAL MODEL

The propagation of a two-dimensional wave packet is examined by solving the fully nonlinear, nonhydrostatic equations of motion with specified initial conditions for the wave packet structure and the background profiles of horizontal velocity $U(z)$ and density $\overline{\rho}(z)$. The numerical model is described in detail in Sutherland;[7] only the salient features are given below. Throughout this paper it is assumed that the flow is uniformly stratified, that is, the background squared buoyancy frequency, $N_\star^2 = -(g/\rho_{00})d\overline{\rho}/dz$, is constant. Here g is the gravitational acceleration and ρ_{00} is a reference value of density. The Boussinesq approximation is used, so that the background density profile can be written as $\overline{\rho}(z) = \rho_{00} - \Delta\rho z/H$, in which H is the height of the domain and $\Delta\rho$ ($\ll\rho_{00}$) is the change in density over this height. Characteristic time ($\mathcal{T}$), length ($\mathcal{L}$), and density ($\Delta\rho$) scales are used to express the equations of motion in nondimensional form. The equations for the vorticity, $\zeta = u_z - w_x$, and perturbation density, ρ, fields are

$$\frac{D\zeta}{Dt} = N_0^2\frac{\partial\rho}{\partial x} + \mathcal{D}_\zeta \tag{1}$$

and

$$\frac{D\rho}{Dt} = w + \mathcal{D}_\rho, \tag{2}$$

in which D/Dt is the material derivative, and u and w are the horizontal and vertical velocity fields, respectively. $N_0 = N_\star\mathcal{T}$ is the nondimensional buoyancy frequency. It has been assumed that density fluctuations occur on the scale $\delta\rho = \mathcal{L}\Delta\rho/\mathcal{H}$, in which case ρ is identical to the nondimensional vertical displacement field, ξ. In order to approximate the motion of inviscid waves while keeping the code numerically stable, the diffusion of the vorticity, $\mathcal{D}_\zeta$, acts only on scales smaller than the horizontal wave number of the wave packet. On these small length scales $\mathcal{D}_\zeta = 1/\mathrm{Re}\nabla^2\zeta$. Likewise, the diffusion of the perturbation density field acts only on small length scales in which case $\mathcal{D}_\rho = 1/\mathrm{Re}\ \mathrm{Pr}\nabla^2\rho$. The Reynolds number is set to $\mathrm{Re}=1000$ and the Prandtl number to $\mathrm{Pr}=1$. Equations (1) and (2) are solved in a horizontally

This article is copyrighted as indicated in the article. Reuse of AIP content is subject to the terms at: http://scitation.aip.org/termsconditions. Downloaded to IP: 129.128.216.34 On: Sun, 23 Mar 2014 03:22:20

periodic channel with free slip boundary conditions using a mixed spectral-infinite difference code developed originally by Smyth and Peltier.[12]

The vertical extent of the domain ranges from $-100 \leqslant z \leqslant 100$. For horizontally periodic internal waves, the horizontal extent of the domain, L_x, is set to be exactly one wavelength. For horizontally compact wave packets, the horizontal extent is set to be $L_x = 64\pi \simeq 201$. Typically, this is 10 to 20 times wider than the width of the wave packets studied. As confirmed by doubling the width of the domain, the periodic boundary conditions have a negligible effect upon the evolution of the wave packet.

The initial wave packet is vertically localized. Over the extent that the amplitude of the initial wave packet is non-negligible, the background flow is stationary. Explicitly, the initial wave packet is prescribed in terms of the stream function $\psi(x,z)$,

$$\psi(x,z) = \Psi(x,z)\exp[\,\iota(k_x x + k_z z)\,] + c.c. \tag{3}$$

In simulations of horizontally periodic internal waves, the envelope of the wave packet is given by

$$\Psi_{\mathrm{PW}}(x,z) = A_0 \exp(-|z-z_0|/\sigma_z). \tag{4}$$

In simulations of horizontally compact wave packets,

$$\Psi(x,z) = A_0 \exp(-|z-z_0|/\sigma_z)\exp(-x^2/2\sigma_x^2). \tag{5}$$

Here the amplitude is A_0, and σ_x and σ_z are the horizontal and vertical extents, respectively, of the wave packet. For finite σ_x and σ_z, and small-amplitude A_0, the initial wave packet defined by Eq. (3) and either (4) or (5) may be thought of as the superposition of monochromatic waves spanning a broad frequency range centered about a frequency ω, determined from the wave number vector (k_x, k_z). The frequency ω is to be estimated from the dispersion relationship for internal waves

$$\omega = N_0 k_x / \sqrt{k_x^2 + k_z^2}. \tag{6}$$

If $1/\sigma_x \ll k_x$ and $1/\sigma_z \ll K_z$ (as in the case in all the studies presented here), the frequency range is sharply peaked about ω and, for a small-amplitude wave packet, linear theory may be applied to it as if it were monochromatic.

The qualitative results presented here are not sensitively dependent upon the form of the wave packet envelopes given by Eqs. (4) and (3). The vertical structure of the envelope is set to be exponential because this corresponds to the structure of a growing and decaying wave packet. For horizontally compact wave packets, the horizontal structure of the envelope is set to be Gaussian in order to be representative of a statistical ensemble of waves with wave number spectrum centered k_x.

For simplicity, the length scale is chosen so that $k_x = 1$ and the time scale is chosen so that $N_0 = 1$. In the Boussinesq approximation, there is no difference in the behavior of upward and downward propagating wave packets. However, to be consistent with studies of internal waves propagating downward from the ocean surface,[13] the internal waves are prescribed initially with positive vertical wave number so that the waves propagate downward.

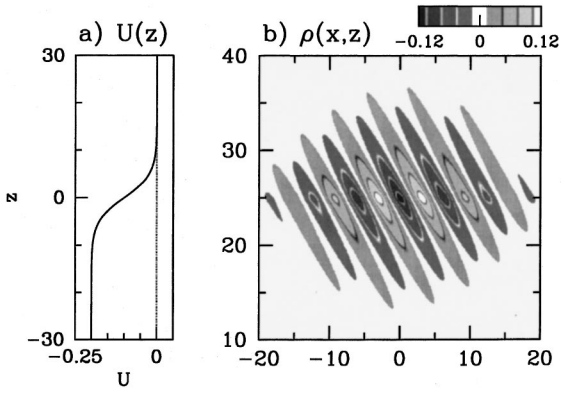

FIG. 1. The (a) background horizontal velocity profile and (b) perturbation density field of an initial wave packet in a typical simulation.

Studies are performed only for wave packets with vertical wave number $k_z = \sqrt{2}/2 \simeq 0.71$. This value is chosen because, with $k_x = 1$, periodic internal waves propagate downward with the largest group velocity $c_{gz} = -2/3\sqrt{3} \simeq -0.38$. In this case $\omega = \sqrt{2/3} \simeq 0.82$. From linear theory, an estimate of the initial amplitude of the vertical displacement field is found to be $A_\xi \simeq 2.45 A_0$. Thus with $A_0 = 1$, for example, the maximum initial vertical displacement is approximately 39% of the horizontal wavelength. The vertical extent of the wave packet is also fixed with $\sigma_z = 5$, so that approximately one vertical wavelength spans the depth of the wave packet. The width σ_x and amplitude A_0 are allowed to vary. As the wave packet propagates downward into flow moving at speed $U(z)$, linear theory predicts that the waves are Doppler-shifted with frequency $\Omega(z) = \omega - k_x U(z)$.

The background flow is defined by

$$U(z) = U_1[1 - \tanh(z/D)]/2, \tag{7}$$

in which U_1 is the flow speed well below the initial wave packet and D is the depth over which the background changes from stationary flow above $z = 0$ to flow moving at speed U_1 below $z = 0$. Throughout we set $D = 5$. The wave packet encounters a reflecting level if U_1 is sufficiently negatively large. Explicitly, this occurs if $U_1 < \sqrt{2/3} - 1 \simeq -0.18$.

The coordinate system is chosen so that the flow changes about $z = 0$, and the wave packet is centered initially about $(x_0, z_0) = (0,25)$. Thus the wave packet is sufficiently close to the region where the background flow changes, but the initial wave packet amplitude near $z = 0$ is negligible.

Typically, simulations are run for times between $t = 0$ and 200. From linear theory, we estimate that the wave packet propagates a total vertical distance of $z \simeq 76$ at the end of a simulation. Therefore, the vertical extent of the domain is sufficiently large that the wave packet has negligibly small amplitude near the top and bottom boundaries throughout the simulation.

Figure 1 shows a typical initial condition for the simulations. Figure 1(a) shows the horizontal velocity profile $U(z)$ with $D = 5$, and $U_1 = -0.2$. In this case, the Doppler-shifted frequency of the wave packet as it propagates well below $z = 0$ is $\Omega \simeq 1.02$, and therefore a reflecting level exists near

This article is copyrighted as indicated in the article. Reuse of AIP content is subject to the terms at: http://scitation.aip.org/termsconditions. Downloaded to IP: 129.128.216.34 On: Sun, 23 Mar 2014 03:22:20

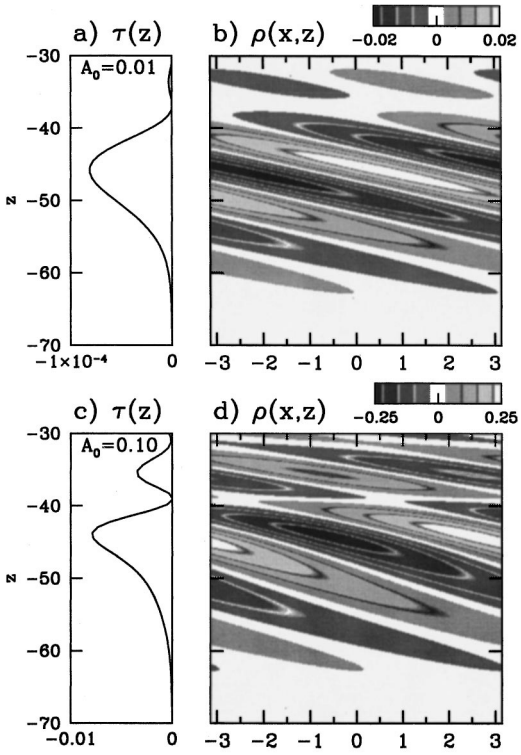

FIG. 2. The (a) Reynolds stress profile and (b) perturbation density field associated with a horizontally periodic wave packet with $A_0=0.01$ in a control simulation at time $t=200$. Diagrams (c) and (d) show the corresponding plots for a wave packet with $A_0=0.10$.

$z=0$ in this case. Figure 1(b) shows the perturbation density field $\rho(x,z)$ of an initial wave packet with amplitude $A_0=0.04$ and horizontal extent $\sigma_x=10$. The down and rightward tilt of the phase lines is consistent with the structure of internal waves that propagate downward to the right.

III. RESULTS

Here the results are presented of control simulations examining the propagation of wave packets in uniformly stratified, stationary flow. These simulations serve to demonstrate how nonlinearity affects the propagation and dispersion of the waves. Following this the results are presented of a range of simulations performed to examine the behavior of internal waves incident upon a level in a background shear flow where $\Omega/N_0\simeq 1$. The effect of varying the initial amplitude and horizontal extent of the wave packet is examined.

A. Control simulations

The effect of nonlinearity upon the dispersion of internal waves is demonstrated by comparing the behavior of small- and large-amplitude wave packets. The structure of horizontally periodic wave packets at time $t=200$ in a simulation are shown in Fig. 2. Figure 2(a) shows the vertical profile of the Reynolds stress per unit mass, $\tau(z)=\langle u'w'\rangle$, in which u' and w' are the perturbation horizontal and vertical velocities, respectively, and the angle brackets denote the domain horizontal average. The profile is shown for a simulation of a small-amplitude wave packet with $A=0.01$. The Reynolds stress is negative over the extent of the wave packet as expected for a wave packet that transports forward momentum downward. Figure 2(b) shows the corresponding perturbation density field, $\rho(x,z)$, at the same time. Although there has been weak wave dispersion, the diagram demonstrates that the extent of the wave packet and the tilt of the phase lines are approximately the same as those of the initial wave packet. The centroid position of the wave packet is calculated from the weighted average of the momentum flux using only values within 95% of the minimum value of τ. The width is standard deviation of this normalized distribution. At time $t=0$ the wave packet is found to be centered at $z=25.0$, as expected. The width of the wave packet is 3.7, moderately smaller than the e-folding depth, $\sigma_z=5$. At time $t=200$ the wave packet is centered at $z\simeq -47.2$ with width 4.3. According to linear theory, small-amplitude waves are expected to propagate downward at the speed of the vertical group velocity $c_{gz}\simeq -0.38$. Thus at time $t=200$, the wave packet is expected to be localized about $z=-51$, which is moderately deeper than its observed position. This discrepancy occurs because the initial wave packet, being vertically compact, is the superposition of internal waves with a range of vertical wavelengths centered about $k_z=\sqrt{2}/2$. Thus the wave packet is expected to propagate with vertical velocity moderately less than c_{gz}.

As in Figs. 2(a) and 2(b), Figs. 2(c) and 2(d) show the Reynolds stress profile and perturbation density field, respectively, at time $t=200$ for a simulation of a large-amplitude wave packet with $A_0=0.10$. In this case, the dispersion of the wave packet is more pronounced. The Reynolds stress profile shows multiple peaks, though the peak at the leading edge is largest. For this leading peak, the centroid position is at $z\simeq -46.5$ and the width of the peak is 4.1. The centroid of the wave packet including the trailing peaks is at $z\simeq -44.2$ with width 6.1. Thus the effect of weak nonlinearity associated with the large-amplitude wave packet is to moderately reduce the average vertical speed of propagation of the wave packet and to enhance its dispersion.

In comparison with horizontally periodic wave packets, simulations have been performed of horizontally and vertically compact wave packets in uniformly stratified stationary flow. As in Fig. 2, Fig. 3 shows the Reynolds stress profiles and perturbation density fields at time $t=200$ taken from simulations of small- and large-amplitude wave packets. The initial horizontal width of both wave packets is $\sigma_x=10$. Figures 3(a) and 3(b) show the structure of a small-amplitude wave packet with $A_0=0.04$. The wave packet undergoes greater dispersion compared with that of the horizontally periodic wave packet. At time $t=200$, the peak amplitude of the perturbation density field is $|\rho'|\simeq 0.04$, which is almost one-third the peak amplitude at time $t=0$. The phase tilt of the waves to the left of the wave packet center is more vertical and the phase tilt of the waves to the right is more horizontal. The position of the centroid of the wave packet at this time is $z\simeq -48.8$ with width 6.6. Thus the wave packet is approximately 80% wider than the small-amplitude horizontally periodic wave packet shown in Fig. 2(b). The average vertical speed is approximately the same in both cases.

Figure 3(c) shows the Reynolds stress profile and Fig. 3(d) shows the perturbation density field at time $t=200$ of a

This article is copyrighted as indicated in the article. Reuse of AIP content is subject to the terms at: http://scitation.aip.org/termsconditions. Downloaded to IP: 129.128.216.34 On: Sun, 23 Mar 2014 03:22:20

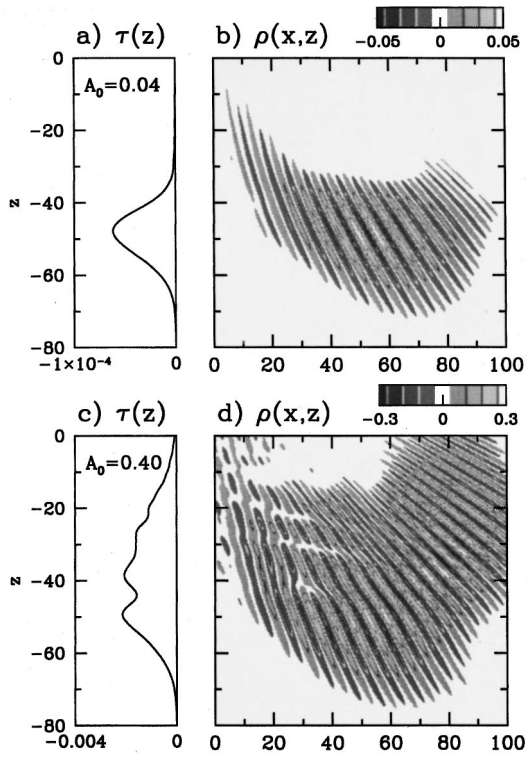

FIG. 3. As in Fig. 2 but for compact wave packet with width $\sigma_x = 10$ and in (a) and (b) $A_0 = 0.04$, and in (c) and (d) $A_0 = 0.40$.

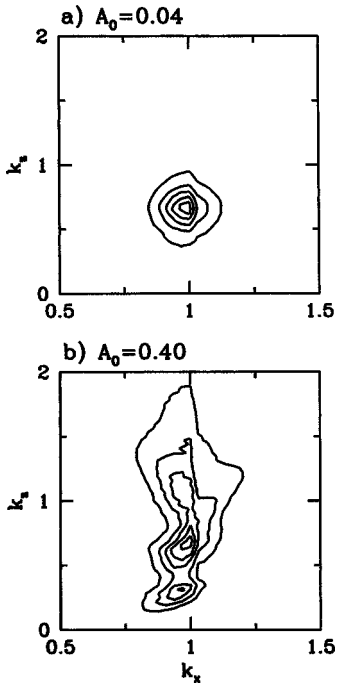

FIG. 4. Normalized power spectra of (a) small-amplitude and (b) large-amplitude compact wave packets at time $t = 200$, computed from perturbation density fields shown in Figs. 3(b) and 3(d), respectively. Contours are shown by intervals of 0.2.

large-amplitude wave packet with $A_0 = 0.40$. The dispersion of the wave packet is significant in this case. The wave packet has both broad vertical and horizontal extents. The position of the centroid of the wave packet is $z \simeq -38.2$ and its width is 14.1. Thus, among other effects, nonlinearity acts to significantly slow the vertical speed of propagation of the wave packet, and this effect is much more pronounced if the wave packet is horizontally compact. As discussed below, this is a consequence of the wave–wave interactions that act nonuniformly over the extent of the wave packet to locally change the phase speed of the waves.

B. Wave self-acceleration

The effect of weak nonlinearity upon the spectrum of the wave packet is shown in Fig. 4, which contains contour plots of the normalized power spectrum of the (a) small-amplitude ($A = 0.04$) and (b) large-amplitude ($A = 0.40$) wave packets shown in Figs. 3(b) and 3(d), respectively. The power spectrum is computed from the square of the components of the two-dimensional discrete Fourier transforms of the perturbation density fields. The result is normalized by its maximum value. The contours in both figures range from 0.1 to 0.9 by an interval of 0.2. Figure 4(a) shows that the internal wave spectrum for the small-amplitude wave packet is sharply peaked about wave number vector $(k_x, k_z) \simeq (1.0 \pm 0.06,\ 0.69 \pm 0.12)$, close to the wave number vector (1, 0.71) prescribed to the wave packet at time $t = 0$. The horizontal and vertical widths in wave number space (0.06 and 0.12, respectively) are determined from the standard deviation of the power spectrum calculated for values within 95% of the peak value. The spectrum shown in Fig. 4(b) of the large-amplitude wave packet at time $t = 200$ is much broader. The horizontal wave number is centered about $k_x \simeq 1.0 \pm 0.06$, the width about the peak being comparable to that of the small-amplitude case. However, the vertical wave number spectrum is more broadly distributed with mean $k_z \simeq 0.97 \pm 0.47$. The spectrum exhibits two strong peaks near $k_z \simeq 0.7$ and $k_z \approx 0.3$, and a smaller peak with $k_z \simeq 1.1$. The power spectrum is greater than 0.1 for values of k_z ranging from 0.1 to 1.9. This range is three times larger than the corresponding range in the small-amplitude case. Because the wave number spectrum is broader, the frequency spectrum is also broader. Linear theory is used to estimate the frequency of the waves from the wave number vector. The frequency of the waves with peak power at $(k_x, k_z) = (1, 0.3)$ is 0.96, at $(k_x, k_z) = (1, 0.7)$ is 0.82, and at $(k_x, k_z) = (1, 1.1)$ is 0.67. Thus, if the background flow, $U(z)$, is not uniform but changes according to Eq. (7) with U_1 negative, then the proportion of the wave packet that reflects is expected to be different for large-amplitude and small-amplitude waves. This amplitude-dependent behavior is the result of weakly nonlinear interactions between the waves and the wave-induced mean flow, otherwise known as the self-acceleration of the waves.[8,9]

As shown by Sutherland,[7] the wave-induced mean flow for horizontally periodic internal waves in uniformly stratified fluid is given approximately by the mean horizontal wave pseudomomentum,[14]

$$\overline{U} \simeq \mathcal{M} = -\overline{\zeta' \xi'}, \tag{8}$$

in which ζ' and ξ' are the perturbation vorticity and vertical

This article is copyrighted as indicated in the article. Reuse of AIP content is subject to the terms at: http://scitation.aip.org/termsconditions. Downloaded to IP: 129.128.216.34 On: Sun, 23 Mar 2014 03:22:20

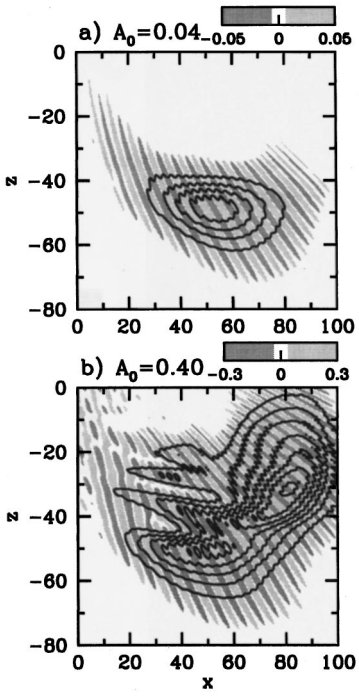

FIG. 5. Contours of $-\overline{\zeta'\xi'}^{\lambda x}$ field (black lines) for (a) small-amplitude and (b) large-amplitude compact wave packet in control simulation at time $t=200$. The contours are superimposed on perturbation density fields (gray-scale) which are reproduced from Figs. 3(b) and 3(d), respectively. Contours are shown by intervals of (a) 0.0002 and (b) 0.005.

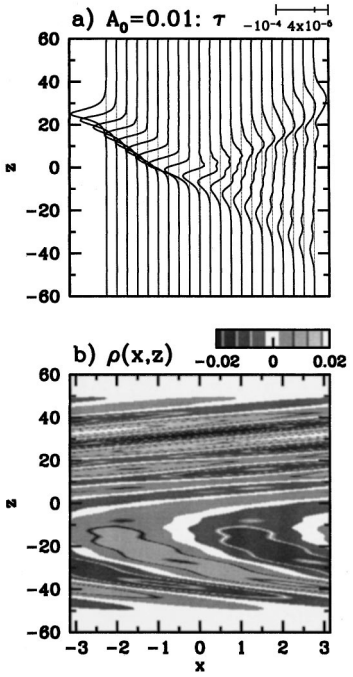

FIG. 6. In (a) a sequence of offset Reynolds stress profiles at times $t=0,10,\ldots,200$, and in (b) the perturbation density field at $t=200$ from a simulation of small-amplitude horizontally periodic wave packet incident upon a reflecting level.

displacement fields, respectively. This estimate is accurate to $O(A_0^3)$. The wave pseudomomentum is well defined for horizontally periodic flows. For compact waves, the effect of self-acceleration is demonstrated by calculating the $\zeta'\xi'$ field and at each point in the field calculating the horizontal average over one wavelength, $\lambda_x=2\pi$: $-\overline{\zeta'\xi'}^{\lambda_x}$. The result is shown in Fig. 5 from simulations at time $t=200$ for (a) small-amplitude ($A=0.04$) and (b) large-amplitude ($A=0.40$) wave packets in stationary, uniformly stratified fluid. The gray scale shows the perturbation density field at this time, reproduced from Figs. 3(b) and 3(d). Superimposed on these are contours of $-\overline{\zeta'\xi'}^{\lambda_x}$. The undulations in the contours are an artifact of the averaging procedure. Nonetheless, the large-scale features give an adequate representation of where the wave-induced flow is significant. In Fig. 5(a) the contours are shown by intervals of 0.0002, the peak value occurring near the center of the wave packet at $(x,z)\simeq(55,-50)$ with value $\bar{U}\simeq 0.001$. In Fig. 5(b) the contours are shown in intervals of 0.005. In this case, there are two peak values occurring near $(x,z)\simeq(55,-50)$ with value $\bar{U}\simeq 0.025$, and near $(80,-30)$ with value $\bar{U}\simeq 0.035$. From linear theory, the group velocity of the initial wave packet is estimated to be $(c_{gx},c_{gz})\simeq(0.27,-0.38)$. Thus, the wave-induced mean flow of the large-amplitude wave packet is as large as 10% of the horizontal group velocity and, therefore, has an arguably significant impact upon the wave packet evolution.

From the group velocity, the position of the wave packet at time $t=200$ is estimated to be approximately $(54,-51)$. This is comparable to the observed position of the small-amplitude wave packet, and also to the position of the lower peak value of $\bar{U}$ of the large-amplitude wave packet. It is interesting to note that the position of the stronger peak value of $\bar{U}$ is consistent with that expected for a wave packet with the largest horizontal group velocity for which $(k_x,k_z)=(1/\sqrt{2})$ and $(c_{gx},c_{gz})\simeq(0.38,-0.27)$. A detailed analysis of the division of an initial large-amplitude wave packet into parts is currently under investigation, but beyond the scope of this paper.

C. Periodic internal waves in a shear flow

Here the propagation of a horizontally periodic wave packet is examined as it propagates downward through a uniformly stratified shear flow. The background flow has zero speed over the depth of the initial wave packet and has uniform and negative speed at great depths. Because the initial wave packet has positive horizontal phase speed, the Doppler-shifted frequency of the wave packet, $\Omega=\omega-c_{px}U$, becomes larger as it propagates downward. If Ω equals the buoyancy frequency $N_0=1$ at some depth, then the wave packet encounters a reflecting level. For small-amplitude internal waves, it is found that the wave packet is partially reflected from and transmitted across a reflecting level due to transient effects.[7]

Figure 6 shows the results of a simulation of a small-amplitude wave packet, with $A_0=0.01$, propagating through fluid in which the background velocity is given by Eq. (7) with $U_1=-0.2$. In this case the Doppler-shifted frequency of the wave packet well below $z=0$ is $\Omega_1\simeq 1.02>N_0$. Therefore, a reflecting level exists near $z=0$. Figure 6(a)

This article is copyrighted as indicated in the article. Reuse of AIP content is subject to the terms at: http://scitation.aip.org/termsconditions. Downloaded to IP: 129.128.216.34 On: Sun, 23 Mar 2014 03:22:20

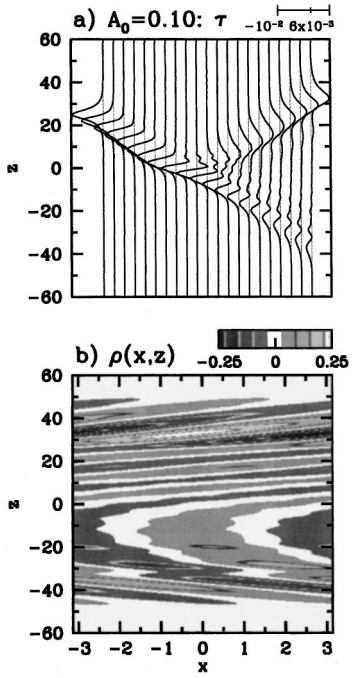

FIG. 7. As in Fig. 6 but for a large-amplitude periodic wave packet.

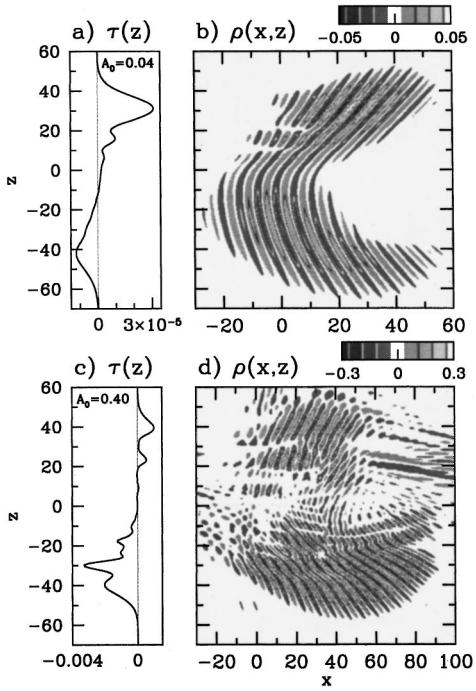

FIG. 8. The (a) Reynolds stress profile and (b) perturbation density field at time $t=200$ from simulation of a small-amplitude horizontally compact wave packet of width $\sigma_x=10$. Diagrams (c) and (d) are the corresponding plots from a simulation of a large-amplitude wave packet.

shows a horizontally offset sequence of profiles of the Reynolds stress, $\tau(z)$. From left to right, the profiles are shown at times $t=0,10,\ldots,200$. Each profile is shown on a scale ranging from -10^{-4} to 4×10^{-5}. Initially, τ is negative about a peak centered at $z=25$. The sign of τ is consistent with the downward transport of forward momentum by the propagating wave packet. It encounters the reflecting level near $z\simeq0$ around time $t\simeq80$ and then proceeds to split into two wave packets, one that continues to propagate downward with an associated negative Reynolds stress [$\tau(z)<0$ for $z<0$], and one that propagates upward with an associated positive Reynolds stress [$\tau(z)>0$ for $z>0$]. Figure 6(b) shows the perturbation density field at $t=200$ in this simulation. The contours in the diagram range between -0.02 and 0.02. The diagram shows two wave packets, which can be distinguished from the tilt of the phase lines above and below $z=0$. The right and downward tilt of the waves below $z=0$ is consistent with their expected downward propagation. By calculating the position of the centroid of the perturbation kinetic energy associated with the wave packet with negative Reynolds stress, the wave packet is found to be centered about $z\simeq-33.7$ with width 7.8. The right and upward tilt of the waves above $z=0$ is consistent with upward propagation. These waves are centered about $z\simeq27.3$ with width 10.0.

For comparison, a simulation is performed with the same initial background flow but for a large-amplitude wave packet with $A_0=0.10$. As in Fig. 6, Fig. 7(a) shows a sequence of profiles of $\tau(z)$, each profile shown on a scale ranging from -10^{-2} to 6×10^{-3}. As in the small-amplitude, case, the wave packet encounters the reflecting level near $z=0$ and splits into a transmitted, downward propagating and reflected, upward propagating wave packet. By comparison, the vertical width of both wave packets at late times is moderately smaller. Figure 7(b) shows the perturbation density field associated with the waves at time $t=200$. The contours range from -0.25 to 0.25. As before, it is found that the tilt of the phase lines below $z=0$ is downward and to the right. This downward propagating wave packet is centered about $z\simeq-34.0$ with width 7.2. The upward propagating wave packet above $z=0$ is centered about $z\simeq32.2$ with width 6.3.

Nonlinear effects act to reduce the width of the wave packet and to increase its vertical group velocity. As will be shown in Sec. IV, nonlinearity also acts to increase or decrease the proportion of the wave packet that is reflected.

D. Compact internal waves in a shear flow

As discussed above, horizontal and vertical wave dispersion can be enhanced for large-amplitude compact wave packets due to wave self-acceleration. When a compact wave packet encounters a reflecting level, the superposition of the incident and reflected wave packets effectively increases the amplitude of the waves and thus the dispersion of the waves is further enhanced. Here the effect of this dispersion upon the structure of the reflected and transmitted waves is qualitatively examined.

Figure 8 shows the results at time $t=200$ of two simulations of the propagation of small- and large-amplitude compact wave packets. In both cases the horizontal width is $\sigma_x=10$. As in the simulations of horizontally periodic internal waves discussed above, the background flow speed is given by Eq. (7) with $U_1=-0.2$. Thus the Doppler-shifted frequency of the wave packet well below $z=0$ is $\Omega\simeq1.02$, and so a reflecting level exists near $z=0$. Figure 8(a) shows the Reynolds stress profile at $t=200$ for a simulation of a

This article is copyrighted as indicated in the article. Reuse of AIP content is subject to the terms at: http://scitation.aip.org/termsconditions. Downloaded to IP: 129.128.216.34 On: Sun, 23 Mar 2014 03:22:20

small-amplitude wave packet with $A_0=0.04$. Figure 8(b) shows the corresponding perturbation density field over the same vertical extent. Only a fraction of the horizontal extent of the computational domain is shown. Contours range between -0.05 and 0.05. Due to the horizontal dispersion of the wave, the peak perturbation density is less than half that of the peak value at time $t=0$.

The wave packet below $z=0$ has right and downward-tilting phase lines, and the Reynolds stress is negative over its vertical extent. These characteristics are consistent with a downward propagating wave packet. From its perturbation kinetic energy profile at this time, the downward propagating wave packet is found to be centered about $z\simeq -40.0$ with width 10.3. Consistent with the properties of upward propagating internal waves, the wave packet above $z=0$ has right and upward-tilting phase lines, and its associated Reynolds stress is positive. It is centered about $z\simeq 28.3$ with width 9.7.

Figure 8(c) shows the Reynolds stress profile for a simulation of a large-amplitude wave packet with $A_0=0.40$. Figure 8(d) shows the corresponding perturbation density field, with contours ranging from -0.3 to 0.3. As in the case with $A_0=0.04$, the diagrams show the transmission and reflection of the wave packet across a reflecting level near $z=0$. In this case, however, the structure and relative amplitude of the wave packets are significantly different. Although initially the amplitude of the large-amplitude wave packet is ten times larger than that of the small-amplitude wave packet, at time $t=200$ the amplitude is only six times larger.

The horizontal extent of the wave packet is much broader. Below $z=0$ its half width is approximately 25, compared with that of the small-amplitude wave packet, which is approximately 17. The Reynolds stress associated with the downward propagating wave packet has multiple peaks and the magnitude of the momentum flux associated with it is significantly larger than the magnitude of the momentum flux of the upward propagating wave packet above $z=0$. The centroid of the wave packet is at $z\simeq -32.1$ with width 9.9, which is not as deep as its counterpart in the simulation of the small-amplitude wave packet [Fig. 8(b)]. Thus the average vertical speed of propagation of the wave packet below $z=0$ is smaller in the large-amplitude case. The centroid of the upward propagating wave packet above the reflecting level is at $z\simeq 36.5$ with width 8.4. This is significantly higher than the depth of its small-amplitude counterpart, and thus the average vertical speed of propagation of the reflected wave packet is larger in the large-amplitude case.

The normalized power spectrum of the transmitted and reflected wave packets is calculated from the perturbation density field as described in Sec. III B. From simulations at time $t=200$ when the transmitted, downward propagating and the reflected, upward propagating wave packets are sufficiently spatially separated, the power spectrum is calculated for the field below and above $z=0$, respectively. Figure 9 shows the power spectrum for the simulations of the small ($A=0.04$) and large ($A=0.40$) amplitude wave packets at time $t=200$. The corresponding perturbation density fields are shown in Figs. 8(b) and 8(d), respectively. In each case the contours are shown in intervals of 0.2 ranging from 0.1 to

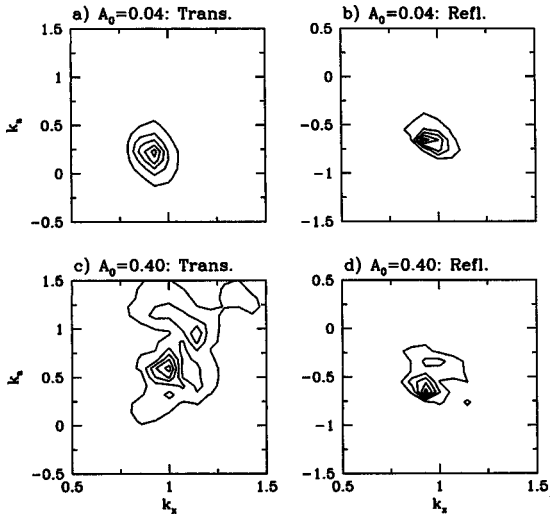

FIG. 9. Normalized power spectra of (a) transmitted and (b) reflected small-amplitude wave packet computed from perturbation density fields shown in Fig. 8(b). Diagrams (c) and (d) show the corresponding plots computed for a large-amplitude wave packet, the perturbation density field of which is shown in Fig. 8(d).

0.9. Figure 9(a) shows the power spectrum of the transmitted small-amplitude wave packet. The peak power occurs at wave number $(k_x,k_z)\simeq(0.96\pm 0.5,0.27\pm 0.14)$. From linear theory, this corresponds to a Doppler-shifted frequency of $\Omega\simeq 0.96$, close to the background buoyancy frequency $N=1$. The horizontal wave number is 4% smaller than that of the wave packet at time $t=0$. Figure 9(b) shows the power spectrum of the reflected small-amplitude wave packet. For these waves, the power is sharply peaked about $(k_x,k_z)\simeq(0.96\pm 0.06,-0.63\pm 0.09)$. The corresponding frequency is comparable to the frequency of the initial wave packet.

Figure 9(c) shows the power spectrum of the transmitted large-amplitude waves. The peak in the power spectrum occurs for wave numbers about $(k_x,k_z)\simeq(1.04\pm 0.5,0.63)$. The width of the vertical wave number spectrum is much broader than the small-amplitude case. However, the horizontal wave number spectrum remains sharply peaked. The weighted mean power occurs for $k_z\simeq 0.90$ with standard deviation 0.33. The power spectrum of the reflected large-amplitude wave packet is shown in Fig. 9(d). Here the peak power occurs about $(k_x,k_z)\simeq(0.96\pm 0.05,-0.63)$, and the weighted mean power occurs for $k_z\simeq -0.48$ with standard deviation 0.16.

Thus, while nonlinear effects do not act to change the horizontal wave number spectrum significantly, the vertical wave number spectrum and the frequency vary greatly. It is interesting to note that for the large-amplitude wave packet, the absolute values of the peak vertical wave numbers of the reflected and transmitted wave packets are comparable and close to the value of the vertical wave number of the initial wave packet.

In both the small- and large-amplitude cases incident upon a region where $\Omega>N$, the power associated with the transmitted wave packet is significant only for positive values of k_z. That is, the waves are not evanescent, but downward propagating. For small-amplitude waves, the reflecting

This article is copyrighted as indicated in the article. Reuse of AIP content is subject to the terms at: http://scitation.aip.org/termsconditions. Downloaded to IP: 129.128.216.34 On: Sun, 23 Mar 2014 03:22:20

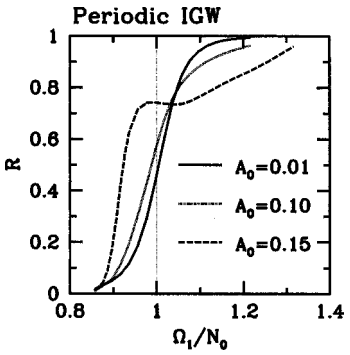

FIG. 10. The reflection coefficient as a function of Ω_1/N_0 for periodic wave packets of amplitude $A_0=0.01$ (solid line), $A_0=0.10$ (short-dashed line), and $A_0=0.15$ (long-dashed line).

level acts as a filter that removes the proportion of the wave packet associated with Doppler-shifted frequencies larger than N. For large-amplitude waves, this filtering acts in conjunction with nonlinear effects that distort the spectrum of the initial wave packet.

IV. REFLECTION COEFFICIENTS

To quantify the degree to which incident waves reflect, the reflection coefficient, $\mathcal{R}$, is calculated, this acting as a measure of the proportion of the wave packet that is propagating upward at time $t=200$. Explicitly, $\mathcal{R}$ is defined as the ratio of the integral of the perturbation kinetic energy above $z=0$ to the integral of this energy over the whole domain. Though not shown here, the reflection coefficient has also been calculated in terms of the total energy (i.e., the perturbation kinetic and available potential energy) and, for horizontally periodic waves, in terms of the wave pseudomomentum. The calculated reflection coefficient is approximately the same in each case. Plots of the evolution of the reflection coefficient in time (not shown here) demonstrate that $\mathcal{R}$ changes by less than 5% between times $t=150$ and 200.

Figure 10 shows the reflection coefficient of horizontally periodic internal waves as a function of the ratio of the Doppler-shifted frequency of the wave packet in the deep fluid, $\Omega_1=\omega-k_xU_1$, to the buoyancy frequency $N_0=1$. If $\Omega_1/N_0>1$, then the initial wave packet encounters a reflecting level near $z=0$. From linear theory, plane periodic (i.e., monochromatic) internal waves are expected to reflect entirely from this level, so that $\mathcal{R}=1$. Likewise, if $\Omega_1/N_0<1$, from linear theory plane periodic waves are expected to transmit entirely so that $\mathcal{R}=0$. However, because the vertical extent of the wave packets in the simulation is finite, the waves are not monochromatic. Indeed, for a small-amplitude wave packet with $A_0=0.01$ (solid line), the reflection coefficient is significantly less than 1 for $1<\Omega_1/N_0<1.1$, and $\mathcal{R}\gg 0$ for $0.9<\Omega_1/N_0<1$. Sutherland[13] has shown that the form of this curve is well predicted by linear theory that takes into account the initially broad power spectrum of the simulated waves.

If the initial wave packet is of large amplitude, the proportion of the initial wave packet that is reflected is less than that predicted by linear theory if $\Omega_1/N_0>1.04$. If $\Omega_1/N_0<1.04$, the proportion of the initial wave packet that is transmitted is greater than that predicted by linear theory.

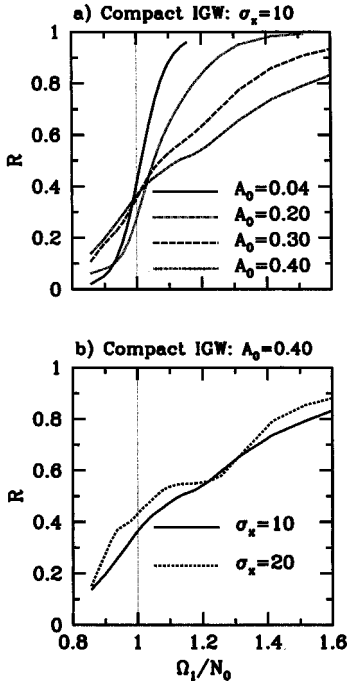

FIG. 11. The (a) reflection coefficient as a function of Ω_1/N_0 for compact wave packets of amplitude $A_0=0.04$ (solid line), $A_0=0.20$ (short-dashed line) and $A_0=0.30$ (long-dashed line), and $A_0=0.40$ (dash-dotted line). (b) Reflection coefficient for large-amplitude compact wave packet with $A_0=0.40$ and width $\sigma_x=10$ (solid line) and $\sigma_x=20$ (dashed line).

As shown above, nonlinear effects significantly broaden the spectrum of a wave packet that is horizontally compact. Figure 11 shows the reflection coefficients as a function of Ω_1/N_0 for simulations of horizontally compact wave packets. In (a) the reflection coefficients are shown for simulations of wave packets with horizontal width $\sigma_x=10$ and a range of amplitudes from $A_0=0.04$ (solid line), to $A_0=0.40$ (dot-dashed line), as indicated on the diagram. When the initial wave packet is of small amplitude (e.g., $A=0.04$), the reflection coefficient as a function of Ω_1/N_0 is similar to that for horizontally periodic internal waves. The curve agrees well with that predicted by linear theory (not shown).

Due to the dispersion of compact wave packets, the amplitude decreases rapidly in time from its initial value. Thus for $A_0<0.10$, the amplitude of the wave at time $t=200$ is so small that the curve $\mathcal{R}(\Omega_1/N_0)$ differs insignificantly from that predicted by linear theory. For larger values of the initial amplitude, enhanced transmission of the wave packet occurs for $\Omega_1/N_0>1$. Indeed, $\mathcal{R}$ is significantly less than 1 over a much greater range than that for horizontally periodic wave packets. For example, if $A_0=0.40$ and $\Omega_1/N_0=1.82$ ($U_1=-1.0$), the reflection coefficient is $\mathcal{R}=0.89$ for a compact wave packet with $\sigma_x=10$, whereas $\mathcal{R}$ is negligibly different from 1 for a periodic wave packet of comparable amplitude at time $t=200$. For $\Omega_1/N_0<1$, the reflection of the incident wave packet is enhanced, though to a lesser degree for compact wave packets than for periodic wave packets.

This article is copyrighted as indicated in the article. Reuse of AIP content is subject to the terms at: http://scitation.aip.org/termsconditions. Downloaded to IP: 129.128.216.34 On: Sun, 23 Mar 2014 03:22:20

Figure 11(b) compares the reflection coefficients for simulations of large-amplitude wave packets ($A_0=0.40$) with horizontal widths $\sigma_x=10$ and 20. The plot shows that the reflection coefficient is generally larger for a wave packet of double the width over the calculated range $0.86<\Omega_1/N_0<1.82$. This result is consistent with the expectation that in the limit of compact wave packets of very large horizontal extent, the reflection coefficient should approach that for horizontally periodic waves. Simulations of wave packets of horizontal extent significantly larger than $\sigma_x=20$ have not been possible due to limitations in the speed and memory of the computational resources available.

V. DISCUSSION AND CONCLUSIONS

Numerical simulations have demonstrated that the amplitude and horizontal extent of a wave packet are significant factors in determining the dynamics of internal waves incident upon a reflecting level. In particular, this work demonstrates that a significantly greater proportion of incident internal waves may be transmitted above a reflecting level than predicted by linear theory. Compared with horizontally periodic waves, an even greater proportion of the incident wave packet is transmitted for a wave packet that is horizontally compact but whose horizontal extent encompasses many wavelengths. For example, linear theory predicts almost 100% reflection of a wave packet with amplitude $A_0=0.40$ that propagates across a shear flow into a region where its Doppler-shifted frequency is 20% greater than the background buoyancy frequency. (For reference, the maximum vertical displacement of this wave packet initially is $A_{\Delta z}\simeq 1$, about 16% of the horizontal wavelength.) In fact, approximately 50% of a wave packet with this amplitude is transmitted below the reflecting level and where it continues to propagate.

At present it is not obvious how the results presented here might be efficiently employed in a general circulation model. In these models and in analytic theories applied to understanding the impact of internal waves upon the large-scale circulation of the atmosphere and ocean, linear theory is frequently employed to estimate at which vertical levels incident internal waves might break or reflect. This approach is beneficial in part because it is easily adapted to speedy computation in numerical models. In many oceanographic and atmospheric circumstances, internal waves have been observed with amplitudes large enough that nonlinear effects play a significant role. The results presented here demonstrate, however, that this methodology should be applied with caution when modeling the dynamics of nonhydrostatic large-amplitude internal waves.

It is worthwhile commenting upon the possibility of applying weakly nonlinear theory to elucidate further the results presented here. Weakly nonlinear evolution equations have been developed by Smith[15] to model the growth in amplitude of surface waves near caustics, and Peregrine and Smith[16] have modeled the weakly nonlinear behavior near caustics of dispersive waves in general. The resulting equations, which have the form of a Nonlinear Schrödinger (NLS) equation, require that the background varies slowly on a scale comparable with the wavelength of the waves. This is not the case for the waves studied here: in order to demonstrate the steady propagation of transmitted and reflected waves, the simulations have been set up so that the background is uniform well above and well below a localized region within which the background flow varies over a length scale comparable with the vertical wavelength of the wave packet.

Weakly nonlinear theory has been applied to examine the resonant over-reflection of internal waves at a critical level (where the phase speed of the wave equals the speed of the background flow) in a thin shear layer.[17] However, these results cannot easily be extended to examine the reflection of waves from a reflecting level because the incident waves cannot couple with an unstable mode of the background flow; the phase speed of the incident waves must lie outside the range dictated by Howard's semicircle theorem.[18]

In order to adapt existing weakly nonlinear theories of waves near caustics to the study of reflecting internal waves, a straightforward first step would be to run a new series of numerical simulations modeling the behavior of internal waves propagating in constant, but weak shear. In these simulations, total reflection of the waves, independent of the initial wave packet amplitude, is anticipated. However, weakly nonlinear effects would act to shift the vertical level at which the waves reflect. This research is currently in progress.

[1]F. P. Bretherton, ''Gravity waves in shear,'' Q. J. R. Meteorol. Soc. **92**, 466 (1966).
[2]K. B. Winters and E. A. D'Asaro, ''Three-dimensional wave instability near a critical level,'' J. Fluid Mech. **272**, 255 (1994).
[3]P. N. Lombard and J. J. Riley, ''On the breakdown into turbulence of propagating internal waves,'' Dyn. Atmos. Oceans **23**, 345 (1996).
[4]M. J. Lighthill, *Waves in Fluids* (Cambridge University Press, Cambridge, 1978).
[5]W. Blumen, ''Reflection of hydrostatic gravity waves in a stratified shear flow. Part i: Theory,'' J. Atmos. Sci. **42**(21), 2255 (1985).
[6]S. D. Eckermann, ''Influence of wave propagation on the Doppler spreading of atmospheric gravity waves,'' J. Atmos. Sci. **54**, 2554 (1997).
[7]B. R. Sutherland, ''Internal gravity wave radiation into weakly stratified fluid,'' Phys. Fluids **8**, 430 (1996).
[8]R. H. J. Grimshaw, ''Nonlinear internal gravity waves and their interaction with the mean wind,'' J. Atmos. Sci. **32**, 1779 (1975).
[9]D. C. Fritts and T. J. Dunkerton, ''A quasi-linear study of gravity-wave saturation and self-acceleration,'' J. Atmos. Sci. **41**, 3272 (1984).
[10]A. Eliassen and E. Palm, ''On the transfer of energy in stationary mountain waves,'' Geofys. Publ. **22**, 1 (1961).
[11]D. G. Andrews and M. E. McIntyre, ''Planetary waves in horizontal and vertical shear: The generalized Eliassen-Palm relation and the mean flow acceleration,'' J. Atmos. Sci. **33**, 2031 (1976).
[12]W. D. Smyth and W. R. Peltier, ''The transition between Kelvin-Helmholtz and Holmboe instability: An investigation of the overreflection hypothesis,'' J. Atmos. Sci. **46**, 3698 (1989).
[13]B. R. Sutherland, ''The dynamic excitation of internal gravity waves in the equatorial oceans,'' J. Phys. Oceanogr. **26**, 3214 (1996).
[14]J. F. Scinocca and T. G. Shepherd, ''Nonlinear wave-activity conservation laws and Hamiltonian structure for the two-dimensional anelastic equations,'' J. Atmos. Sci. **49**, 5 (1992).
[15]R. Smith, ''Giant waves,'' J. Fluid Mech. **77**, 417 (1976).
[16]D. H. Peregrine and R. Smith, ''Nonlinear effects upon waves near caustics,'' Proc. R. Soc. London, Ser. A **292**, 341 (1979).
[17]R. H. J. Grimshaw, ''Resonant over-reflection of internal gravity waves from a thin shear layer,'' J. Fluid Mech. **109**, 349 (1981).
[18]L. N. Howard, ''Note on a paper by John W. Miles,'' J. Fluid Mech. **10**, 509 (1961).

This article is copyrighted as indicated in the article. Reuse of AIP content is subject to the terms at: http://scitation.aip.org/termsconditions. Downloaded to IP: 129.128.216.34 On: Sun, 23 Mar 2014 03:22:20